

the SiC condensation site.

The necessity for large contributions from the He-N zone (70% of the mass making up X57) may indicate that present type II supernova models underestimate the production of ^{26}Al in the H-burning (He-N) zone and also in zones that experienced advanced burning stages. Although the isotopic and elemental abundance pattern of X57 is fully compatible with an origin in a typical type II supernova, those of the majority of the X grains are not. This incompatibility implies either that most X grains injected into the protosolar nebula came from atypical type II supernovae or even from other stellar sources (for example, type I supernovae) or that the production of N, Al, and Si and the layering in presupernova stars is not fully understood by current type II supernova models.

REFERENCES AND NOTES

1. E. Anders and E. Zinner, *Meteoritics* **28**, 490 (1993).
2. S. Amari, P. Hoppe, E. Zinner, R. S. Lewis, *Astrophys. J.* **394**, L43 (1992).
3. P. Hoppe *et al.*, *Lunar Planet. Sci.* **26**, 621 (1995); L. R. Nittler *et al.*, *ibid.*, p. 1057; L. R. Nittler, S. Amari, E. Zinner, S. E. Woosley, R. S. Lewis, *Astrophys. J.*, in press.
4. T. A. Weaver and S. E. Woosley, *Phys. Rep.* **227**, 65 (1993).
5. B. S. Meyer, T. A. Weaver, S. E. Woosley, *Meteoritics* **30**, 325 (1995).
6. S. Woosley and T. A. Weaver, *Astrophys. J. Suppl.* **101**, 181 (1995).
7. S. Amari, R. S. Lewis, E. Anders, *Geochim. Cosmochim. Acta* **58**, 459 (1994).
8. D. D. Clayton, *Nature* **257**, 36 (1975).
9. S. E. Woosley, W. D. Arnett, D. D. Clayton, *Astrophys. J.* **26**, 231 (1973).
10. J. M. Lattimer, D. N. Schramm, L. Grossman, *ibid.* **219**, 230 (1978); J. W. Larimer and M. Bartholomay, *Geochim. Cosmochim. Acta* **43**, 1455 (1979).
11. D. Arnett, B. Fryxell, E. Müller, *Astrophys. J.* **341**, L63 (1989); T. Ebisuzaki, T. Shigeyama, K. Nomoto, *ibid.* **344**, L65 (1989); B. Fryxell, E. Müller, D. Arnett, *ibid.* **367**, 619 (1991); E. Müller, B. Fryxell, D. Arnett, *Astron. Astrophys.* **251**, 505 (1991); M. Herant and W. Benz, *Astrophys. J.* **387**, 294 (1992); M. Herant and S. E. Woosley, *ibid.* **425**, 814 (1994).
12. S. Amari, P. Hoppe, E. Zinner, R. S. Lewis, *Meteoritics* **30**, 679 (1995).
13. T. Shigeyama and K. Nomoto, *Astrophys. J.* **360**, 242 (1990); T. Dotani *et al.*, *Nature* **330**, 230 (1987); S. M. Matz *et al.*, *ibid.* **331**, 416 (1988); W. G. Sandie *et al.*, *Astrophys. J.* **334**, L91 (1988).
14. We gratefully acknowledge the role of E. Anders in the development of separation procedures for presolar SiC grains from meteorites. We also thank S. Woosley for sharing supernova data. This work was supported by the Schweizerischer Nationalfonds zur Förderung der Wissenschaftlichen Forschung and by NASA grant NAGW 3342.

24 October 1995; accepted 5 April 1996

Corundum, Rutile, Periclase, and CaO in Ca,Al-Rich Inclusions from Carbonaceous Chondrites

A. Greshake,* A. Bischoff, A. Putnis, H. Palme

Four calcium,aluminum-rich inclusions from four carbonaceous chondrites—Allende, Acfer 082, Acfer 086, and Acfer 094—were studied by transmission electron microscopy. All inclusions contained at least two of the oxides periclase (MgO), rutile (TiO_2), calcium oxide (CaO), and corundum (Al_2O_3). The oxides (50 to 200 nanometers in size) were found inside and at grain boundaries of the constituent minerals of the inclusions. Determining how these oxides formed may provide insight about condensation processes in the early solar nebula and the origin of refractory inclusions in chondrites. Formation of these oxides by exsolution is considered unlikely. An origin by kinetically controlled condensation appears more probable.

Calcium,aluminum-rich inclusions (CAIs) found in carbonaceous chondrites contain refractory minerals such as spinel, melilite, fassaite, hibonite, grossite, and perovskite (1), mineral phases that may be early condensates from a cooling solar nebular gas (2). The CAIs contain isotopically anomalous oxygen (3), show evidence for the existence

of short-lived nuclides such as ^{26}Al (4), and represent the oldest material formed in the solar system (5). Therefore, CAIs contain valuable information about the very first processes in the solar nebula.

According to thermodynamic calculations (2), corundum was the first solid oxide to condense from the cooling solar nebula. Thus, its mineralogical and textural characteristics are of particular interest for the understanding of the formation of solids in the solar nebula. However, corundum has been identified in very few inclusions [for example, Lancé (6), Murchison (7), and Allende (8)].

Because CAIs are usually studied by

scanning electron microscope, electron microprobe, and ion microprobe, corundum and other simple oxides may not be found, as a result of their small grain size. Therefore, we performed a transmission electron microscopy (TEM) study of four CAIs from different carbonaceous chondrites (9).

Three type A inclusions (10) from Acfer 082, Acfer 086, and Allende (8) and one spinel-perovskite spherule from Acfer 094 were investigated (11, 12). The CAIs were characterized by scanning electron microscopy and electron microprobe and then thinned for TEM studies by conventional ion-beam techniques (13). All phase identifications were made on the basis of compositional analyses and structural characterizations based on selected-area electron diffraction (SAED) patterns.

The CAIs in Acfer 082, Acfer 086, and Allende contain ~70% (by volume) blocky melilite [Åk_{4-13}] crystals that enclose euhedral spinels (15 to 20 volume %, 10 to 80 μm), typically pure MgAl_2O_4 in composition. Fassaite (5 to 10 volume %, 200 to 300 μm) and perovskite (~10 volume %, 50 to 80 μm) occur as irregularly shaped, anhedral grains enclosed within the melilite (14). Some Fe,Ni metals were found in Acfer 082 and Allende CAIs, enclosed within melilite and, more rarely, the spinels. In the Allende CAI, some hibonite laths (20 to 50 μm) and several Os-, W-, and Re-rich particles (up to 60 μm) are present (8). The CAI in Acfer 094 is a 100- μm spinel-perovskite spherule (11). Apart from spinel (~65 volume %) and perovskite (~5 volume %), which are found in the core of the inclusion, the CAI consists of melilite (~10 volume %, Åk_{7-10}) and fassaite (~20 volume %), which basically occur as constituents of the outer layer. All inclusions studied are unweathered, and their interiors do not contain secondary alteration products.

In addition to these mineral phases, we found in all four CAIs oxides that have not been described before and are not predicted to be stable under equilibrium condensation conditions (Table 1). Inclusions of rutile (TiO_2) were identified in CAIs from all four chondrites (Fig. 1A). Energy dispersive spectroscopy (EDS) analyses and SAED confirm that the grains are single crystals and almost pure TiO_2 in composition. As a result of contributions from the surrounding matrix, 50-nm grains contain up to 1 weight % FeO or MgO, or both. The rutile grains range from 50 to 100 nm in size and typically occur as rounded grains located at grain boundaries between spinels and between spinel and perovskite (Fig. 1A). Rarely, the tiny inclusions are embedded within the interiors of the spinels or

A. Greshake and A. Bischoff, Institut für Planetologie, Universität Münster, Wilhelm-Klemm-Straße 10, D-48149 Münster, Germany.

A. Putnis, Institut für Mineralogie, Universität Münster, Corrensstraße 24, D-48149 Münster, Germany.

H. Palme, Mineralogisch-Petrographisches Institut, Universität zu Köln, Zulpicher Straße 49b, 50674 Köln, Germany.

*To whom correspondence should be addressed.

perovskites and show a euhedral to subeuhedral morphology. None of the grains contains any detectable lattice defects like dislocations. No rutile was found in melilite or fassaite.

We found CaO in all four inclusions (Fig. 1D): EDS analyses and SAED patterns prove that the grains have the CaO structure and are pure CaO in composition. The grains are nearly spherical and do not contain any detectable lattice defects (Fig. 1D). The CaO grains are 100 to 200 nm in size and were found embedded in spinel, perovskite, and melilite. They did not occur along grain boundaries.

Periclase (MgO) and corundum (Al_2O_3) were identified only in Acfer 094 (Fig. 1, B and E). In contrast to the type A inclusions, periclase was only found between adjacent spinels. Perovskite, melilite, and fassaite are free of these inclusions (Fig. 1, E and F). Periclase is rare, and the rounded grains (100 to 150 nm) are pure MgO in composition. Inclusions of corundum (100 to 150 nm) are mostly located at the spinel grain boundaries but sometimes were found enclosed within spinel grains (Fig. 1, B and C).

The occurrence of single-oxide mineral grains is unexpected because, except for corundum, simple oxides have condensation temperatures below those of more complex minerals. Simplified calculations of condensation temperatures for each oxide were done assuming a gas of solar composition; thus, depletion of the gas by earlier condensates was not considered (Table 1). The program used for the calculations is described in (15). Thermodynamic data were taken from (16), and solar composition of the gas was assumed in all cases (17). Corundum has the highest condensation temperature, and yet, the mineral is rarely observed in CAIs. The apparent reason is that corundum reacts with the solar gas to form gehlenite and spinel (2). Some of the corundum might not have had sufficient time to react and would be observed today as a relict phase. Rutile condensation temperatures are lower than perovskite conden-

sation temperatures under all conditions. Thus, perovskite is the first Ti-bearing mineral to condense. Under solar nebula oxygen fugacity, TiO_2 and TiO are the major Ti-bearing gas species (17). The abundance of Ti gas is several orders of magnitude lower (16, 17). In contrast, elemental Ca is the major Ca-bearing gas, followed by CaOH (16, 17). Forming a perovskite molecule by condensation thus requires three components: a TiO_2 molecule, a Ca atom, and an O atom. This event may be kinetically more difficult to achieve than the collision of two TiO_2 molecules, although Ca is 10 times more abundant than Ti (17). Thus, this kinetic aspect could delay condensation of perovskite and favor rutile condensation. It should, however, be pointed out that two molecules of TiO_2 are not sufficient to form a rutile crystal; a critical cluster size is required for condensation to take the effect of the surface energy appropriately into account. This critical size requires a certain degree of supersaturation.

However, these effects are probably similar for rutile and perovskite.

Similar arguments may be applied to the condensation of CaO. The fraction of Ca bound in perovskite is about 10%. Most of the Ca will condense as melilite. The equilibrium condensation temperature of melilite is actually lower than the condensation temperatures listed in Table 1 because condensation of corundum depletes the gas in Al. This reduces the difference between the gehlenite and CaO condensation temperatures. The condensation of CaO may well compete with the condensation of such a complex molecule as gehlenite. It is therefore not unreasonable to expect at least some condensed CaO.

The difference in condensation temperatures between MgO and forsterite is only about 50 K (Table 1). It is therefore conceivable that some MgO condenses if equilibrium is not strictly maintained. The effect of kinetic factors that may have influenced condensation depends on the time

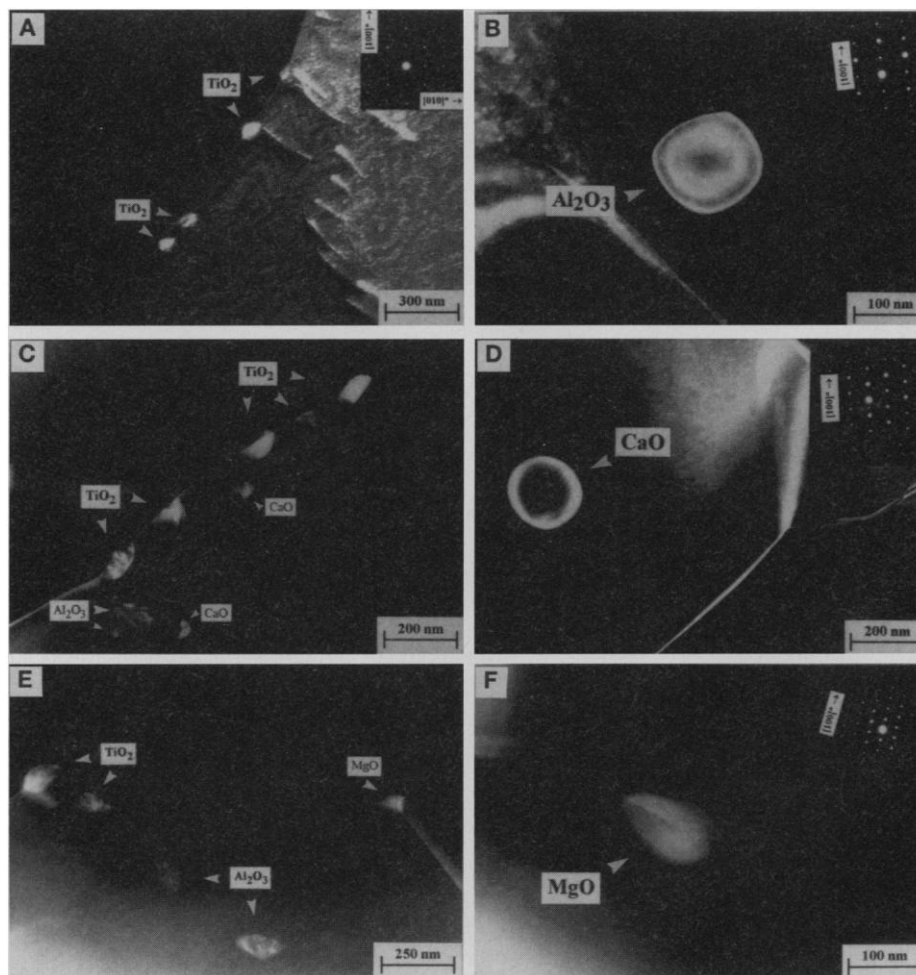


Fig. 1. Dark-field TEM micrographs and SAED patterns of the different oxide inclusions imaged with reflections from the particles only. (A) TiO_2 inclusions at a grain boundary between adjacent spinels from Acfer 082. (B) Al_2O_3 inclusion in spinel from Acfer 094. (C) TiO_2 , Al_2O_3 , and CaO inclusions at a grain boundary between spinels from Acfer 094. (D) CaO inclusion in melilite from Acfer 086. (E) TiO_2 , Al_2O_3 , and MgO inclusions at a grain boundary between adjacent spinels from Acfer 094. (F) MgO inclusion in spinel from Acfer 094.

Table 1. Condensation temperatures for some oxides and silicates at various pressures, assuming solar composition of gas.

| Phase | Condensation temperature (K) at pressure | |
|--------------------------------------|--|---------------|
| | 10^{-3} atm | 10^{-6} atm |
| CaTiO_3 | 1684 | 1471 |
| $\text{Ca}_2\text{Al}_2\text{SiO}_7$ | 1700 | 1493 |
| MgAl_2O_4 | 1675 | 1468 |
| Mg_2SiO_4 | 1443 | 1247 |
| Al_2O_3 | 1762 | 1563 |
| TiO_2 | 1616 | 1425 |
| CaO | 1507 | 1309 |
| MgO | 1395 | 1200 |

scale of cooling. Given comparatively fast cooling, one may even expect that most of the elements condense as single oxides and that they later react with each other to form more complex oxides and silicates. Some of the oxide grains may survive.

Another possibility for the formation of oxide inclusions is grain boundary exsolution within constituents of CAIs if local enrichments of Mg, Ca, Ti, or Al occurred during the crystallization of the host minerals. On the basis of textural observations, such a process seems unlikely. (i) The oxides do not exhibit typical exsolution features. In contrast, some inclusions exhibit euhedral morphologies, which would be unusual for exsolution. (ii) Within an area of 20 nm by 50 nm, three different oxides (TiO₂, CaO, and Al₂O₃) were encountered (Fig. 1C). In the case of diffusion-controlled exsolution, the thermodynamically stable phases CaTiO₃ (perovskite) and CaAl₄O₇ (grossite) would have formed instead of pure oxides. Because exsolution requires the nucleation of a phase so that the resulting two-phase assemblage is more stable than the parent solid solution, it is unlikely that this process leads to the formation of metastable oxide phases. (iii) The exsolution of MgO and Al₂O₃ from spinel; CaO from spinel, perovskite, and melilite; and TiO₂ from spinels and perovskites would be a very unusual phenomenon with no terrestrial equivalent. The range of oxide phases, and in particular the presence of CaO within three different phases, makes it improbable that the oxides were formed by exsolution.

Excluding exsolution as the formation process, we suggest that these inclusions are primary condensates that were either enclosed within or between the host minerals, mostly spinels, and were therefore protected from being consumed by reactions with the remaining solar gas. However, because such phases are not formed by equilibrium condensation, it will be difficult to decipher their formation in detail.

REFERENCES AND NOTES

1. G. J. MacPherson *et al.*, in *Meteorites and the Early Solar System*, J. F. Kerridge and M. S. Matthews, Eds. (Univ. of Arizona Press, Tucson, 1988), pp. 746–807.
2. L. Grossman, *Geochim. Cosmochim. Acta* **36**, 597 (1972).
3. R. N. Clayton, L. Grossman, T. K. Mayeda, *Science* **182**, 485 (1973).
4. C. M. Gray and W. Compston, *Nature* **251**, 495 (1974).
5. G. R. Tilton, in (1), pp. 259–275.
6. G. Kurat, *Earth Planet. Sci. Lett.* **9**, 225 (1970).
7. M. Bar-Matthews, I. D. Hutcheon, G. J. MacPherson, L. Grossman, *Geochim. Cosmochim. Acta* **46**, 31 (1982); G. J. MacPherson, L. Grossman, A. Hashimoto, M. Bar-Matthews, T. Tanaka, *Proc. Lunar Planet. Sci. Conf.* **15**, C229 (1984).
8. A. Bischoff, H. Palme, B. Spettel, *Lunar Planet. Sci.* **XVIII**, 81 (1987).
9. The TEM studies were performed with a 200-kV Philips CM 20 scanning TEM (Institut für Planetologie,

Universität Münster, Germany), equipped with a TRACOR EDAX x-ray detector sensitive to elements with atomic numbers >5, and a JEOL JEM 100 operating at 100 kV (Department of Earth Sciences, University of Cambridge). A thin-film procedure was used in measuring the compositions [G. Cliff and G. W. Lorimer, *J. Microsc.* **103**, 203 (1975)]. Experimental EDS corrections (*K* factors) were derived from analyses of thin-film standards.

10. Type A inclusions consist predominantly of melilite (ÅK_{0–33}) with minor and highly variable proportions of spinel, hibonite, perovskite, and fassaite (1). There is evidence that type A inclusions formed by vapor-solid condensation and were never molten [see, for example, G. J. MacPherson and L. Grossman, *Geochim. Cosmochim. Acta* **48**, 29 (1984); S. B. Simon *et al.*, *Lunar Planet. Sci.* **XXIV**, 115 (1993)].
11. J. Newton *et al.*, *Meteoritics* **30**, 47 (1995).
12. Acfer 082, Acfer 086, and Allende belong to the CV meteorite class [D. W. Sears and R. T. Dodd, in (1), pp. 3–31]. Acfer 094 is a unique primitive carbonaceous chondrite whose mineralogy and oxygen isotopes do not match those of any previously known meteorite class [A. Bischoff and T. Geiger, *Lunar Planet. Sci.* **XXV**, 1309 (1994); (11)]. The CAI in Acfer 082

is 5.2 mm by 2 mm in apparent size; in Acfer 086, 7 mm by 3.5 mm; and in Allende, 8 mm by 3 mm.

13. Samples were ion thinned with a GATAN 600 DIF ion mill at 4.5 kV and 12°.
14. Fassaite in Acfer 082 contains 2.5 to 3.5 weight % TiO₂; in Acfer 086, 2.5 to 4.0 weight %; in Allende, up to 18 weight % (8); and in Acfer 094, 2.0 to 4.5 weight %.
15. H. Palme and B. Fegley Jr., *Earth Planet. Sci. Lett.* **101**, 180 (1990).
16. R. A. Rolie, B. S. Hemingway, J. R. Fisher, *U.S. Geol. Surv. Bull.* **1452** (1979).
17. H. Palme and H. Beer, in *Landolt-Börnstein*, vol. 3, subvol. A of *Group VI Astronomy and Astrophysics*, H. M. Voigt, Ed. (Springer-Verlag, New York, 1993), pp. 196–221.
18. We thank F. Bartschat for photographic work and two anonymous reviewers for their helpful comments. This study was supported by the Deutsche Forschungsgemeinschaft and is part of the thesis of A.G. (Institut für Planetologie, Universität Münster, Germany).

6 February 1996; accepted 18 April 1996

Decline in the Tropospheric Abundance of Halogen from Halocarbons: Implications for Stratospheric Ozone Depletion

Stephen A. Montzka,* James H. Butler, Richard C. Myers, Thayne M. Thompson, Thomas H. Swanson, Andrew D. Clarke, Loreen T. Lock, James W. Elkins

Analyses of air sampled from remote locations across the globe reveal that tropospheric chlorine attributable to anthropogenic halocarbons peaked near the beginning of 1994 and was decreasing at a rate of 25 ± 5 parts per trillion per year by mid-1995. Although bromine from halons was still increasing in mid-1995, the summed abundance of these halogens in the troposphere is decreasing. To assess the effect of this trend on stratospheric ozone, estimates of the future stratospheric abundance of ozone-depleting gases were made for mid-latitude and polar regions on the basis of these tropospheric measurements. These results suggest that the amount of reactive chlorine and bromine will reach a maximum in the stratosphere between 1997 and 1999 and will decline thereafter if limits outlined in the adjusted and amended Montreal Protocol on Substances That Deplete the Ozone Layer are not exceeded in future years.

The Montreal Protocol on Substances That Deplete the Ozone Layer was passed, adjusted, and amended in light of the large body of evidence implicating anthropogenic chlorine- (Cl-) and bromine- (Br-) containing gases in the depletion of stratospheric ozone (O₃) (1–5). Human use of halocarbons has led to a steady increase in the amounts of these compounds in the atmosphere for more than 20 years (6–9). In the modern atmosphere, relatively few halocarbons emitted from natural processes reach the stratosphere (2, 3, 5, 10–12).

Recent reports have highlighted selected anthropogenic halocarbons for which growth rates and abundance have decreased (6–9), owing to restrictions outlined in the Montreal Protocol and its subsequent adjustments and amendments (the revised Montreal Protocol). Model studies have predicted that tropospheric Cl will reach a maximum in the mid-1990s at ~3500 to 4000 pmol mol⁻¹ [parts per trillion (ppt)] if limits outlined in the Copenhagen Amendments are not exceeded (3, 13). These studies further suggest that a minimum for stratospheric O₃ in mid-latitudes will occur 3 to 4 years after the peak in tropospheric Cl and that O₃ abundance will begin to increase as stratospheric Cl concentrations decrease from their maximum. The atmospheric abundance of Br also must be considered, especially because Br is substantially more

S. A. Montzka, J. H. Butler, R. C. Myers, T. M. Thompson, J. W. Elkins, National Oceanic and Atmospheric Administration, Climate Monitoring and Diagnostics Laboratory, Boulder, CO 80303, USA.
T. H. Swanson, A. D. Clarke, L. T. Lock, Cooperative Institute for Research in Environmental Sciences, University of Colorado, Boulder, CO 80309, USA.

*To whom correspondence should be addressed.